



**HAL**  
open science

## Global socioeconomic exposure of heat extremes under climate change

Jie Chen, Yujie Liu, Tao Pan, Philippe Ciais, Ting Ma, Yanhua Liu, Dai Yamazaki, Quansheng Ge, Josep Peñuelas

► **To cite this version:**

Jie Chen, Yujie Liu, Tao Pan, Philippe Ciais, Ting Ma, et al.. Global socioeconomic exposure of heat extremes under climate change. *Journal of Cleaner Production*, 2020, 277, pp.123275. 10.1016/j.jclepro.2020.123275 . hal-02970803

**HAL Id: hal-02970803**

**<https://hal.science/hal-02970803>**

Submitted on 7 Jun 2023

**HAL** is a multi-disciplinary open access archive for the deposit and dissemination of scientific research documents, whether they are published or not. The documents may come from teaching and research institutions in France or abroad, or from public or private research centers.

L'archive ouverte pluridisciplinaire **HAL**, est destinée au dépôt et à la diffusion de documents scientifiques de niveau recherche, publiés ou non, émanant des établissements d'enseignement et de recherche français ou étrangers, des laboratoires publics ou privés.

---

This is the **accepted version** of the article:

Chen, Jie Chen; Liu, Yujie; Pan, Tao; [et al.]. «Global socioeconomic exposure of heat extremes under climate change». *Journal of cleaner production*, Vol. 277 (Dec. 2020), art. 123275. DOI 10.1016/j.jclepro.2020.123275

---

This version is available at <https://ddd.uab.cat/record/232214>

under the terms of the  license

# 2 **Global socioeconomic exposure of heat extremes**

## 3 **under climate change**

4 Jie Chen<sup>1,2</sup>, Yujie Liu<sup>1,2,\*</sup>, Tao Pan<sup>1</sup>, Philippe Ciais<sup>3</sup>, Ting Ma<sup>4</sup>, Yanhua Liu<sup>1</sup>, Dai  
5 Yamazaki<sup>5</sup>, Quansheng Ge<sup>1,2</sup>, & Josep Peñuelas<sup>6,7</sup>

6 <sup>1</sup>Key Laboratory of Land Surface Pattern and Simulation, Institute of Geographic Sciences and  
7 Natural Resources Research, Chinese Academy of Sciences (CAS), Beijing, China

8 <sup>2</sup>University of Chinese Academy of Sciences (UCAS), Beijing, China

9 <sup>3</sup>Laboratoire des Sciences du Climat et de l'Environnement, IPSL-LSCE CEA CNRS UVSQ, Gif-  
10 sur-Yvette, France

11 <sup>4</sup>State Key Laboratory of Resources and Environmental Information System, Institute of  
12 Geographic Sciences and Natural Resources Research, Chinese Academy of Sciences (CAS),  
13 Beijing, China

14 <sup>5</sup>Institute of Industrial Sciences, University of Tokyo, Tokyo, Japan

15 <sup>6</sup>CSIC, Global Ecology CREAM-CSIC-UAB, Bellaterra, 08193 Barcelona, Catalonia, Spain

16 <sup>7</sup>CREAF, Cerdanyola del Vallès, 08193 Barcelona, Catalonia, Spain

17

18 \* Corresponding author at: No.11A, Datun Road, Chaoyang District, Beijing, China

19 E-mail address: liuyujie@igsrr.ac.cn (Yujie Liu)

### 20 **Abstract**

21 Growing evidence indicates that the risk of heat extremes will increase as climate  
22 change progresses and create a significant threat to public health and the economy.  
23 Socioeconomic exposure is the key component for assessing the risk of such events. To  
24 quantify socioeconomic exposure to heat extremes for 2016–2035 and 2046–2065, we  
25 use the projections of five global climate models forced by using three representative  
26 concentration pathways (RCPs) and projections of population and gross domestic  
27 product (GDP), and we take into account the geographic change in the distribution in  
28 shared socioeconomic pathways (SSPs). The exposure of the global population for  
29 2046–2065 is the greatest under the RCP8.5-SSP3 scenario, up to  $1037(\pm 164) \times 10^9$   
30 person-days, and the global GDP exposure for 2046–2065 is greatest under the RCP2.6-  
31 SSP1 scenario, up to  $18(\pm 2) \times 10^{15}$  dollar-days. Asia has the highest exposure among  
32 all continents for both population and GDP, accounting for over half of the global  
33 exposure. Africa has the largest increase in exposure, with the annual population and  
34 GDP exposures increasing by over 9- and 29-fold, respectively, compared with the base  
35 period (1986–2005). The effect of climate makes the dominant contribution (47%–53%)  
36 globally for the change in population exposure. Changes in the geographic distribution  
37 of GDP cause nearly 50% of the total change in GDP exposure for 2016–2035.  
38 Mitigating emissions of greenhouse gases, either at the level of the RCP2.6 scenario or  
39 at a more ambitious target, is essential for reducing socioeconomic exposure to heat

40 extremes. In addition, designing and implementing effective measures of adaptation are  
41 urgently needed in Asia and Africa to aid socioeconomic systems suffering from heat  
42 extremes due to climate change.

43 **Keywords** socioeconomic exposure; heat extremes; climate change; population  
44 exposure; gross domestic product (GDP) exposure

## 45 **1 Introduction**

46 Climatic extremes cause extensive economic damage each year, and the risks are  
47 expected to increase with continued socioeconomic development and climate change.  
48 Risk is usually represented as the probability of occurrence of hazardous events or  
49 trends multiplied by the impact if these events or trends occur. Risk is due to the  
50 interaction of hazard, exposure, and vulnerability. Exposure usually refers to the people,  
51 livelihoods, resources, infrastructure, and economic, social, or cultural assets in places  
52 and settings that could be adversely affected (IPCC, 2014). The prediction of changes  
53 in exposure to future climatic extremes could, therefore, contribute to the need to  
54 consider effective countermeasures to reduce vulnerability and risk. Global  
55 socioeconomic exposure (i.e., exposure of the population and gross domestic product,  
56 GDP) under climate change has received less attention (Burke et al., 2015; Carleton  
57 and Hsiang, 2016), despite recent progress in assessing the hazards of climatic extremes  
58 (Hirabayashi et al., 2013; Cook et al., 2014; King et al., 2017; Huang et al., 2017; Nath  
59 et al., 2017). Such estimates are urgently needed to clarify future spatiotemporal  
60 variation and changes in global socioeconomic exposure and thereby avoid adverse  
61 effects on public health and the economy. The importance of assessing exposure is  
62 gradually being recognized, as indicated by the published reports of the  
63 Intergovernmental Panel on Climate Change (Field et al., 2012; IPCC, 2013), the  
64 proposal of a new set of shared socioeconomic pathways (SSPs, O'Neill et al., 2014),  
65 and some recent studies of the risk of climate change that considers the effects of  
66 socioeconomic factors (Ceola et al., 2015; Mora et al., 2017; Zhang et al., 2018). The  
67 integration of climate change with the social economy to estimate future risk, the  
68 assessment of the relative importance of different factors, and the quantification of  
69 uncertainty would provide a basis for adapting to extreme climate change and reducing  
70 the risk of heat extremes.

71 Because of climate change, the frequency and intensity of climatic extremes, such as  
72 heat extremes, have increased in recent decades and are likely to continue to increase  
73 in the coming decades (IPCC, 2013). Heat extremes have been responsible for  
74 significant public health threats and economic losses over the last 100 years. Data for  
75 historical damage from the International Disaster Database  
76 ([https://www.emdat.be/emdat\\_db/](https://www.emdat.be/emdat_db/)) indicate that heat extremes affected  $1.03 \times 10^8$   
77 people, which includes the deaths of 183495 people, and caused worldwide economic  
78 losses of  $6.33 \times 10^{10}$  USD from 1936 to 2019. Serious heat extremes have also occurred  
79 more frequently in recent decades, such as those in Europe in 2003, 2018 and 2019  
80 (Robine et al., 2008), Australia in 2008 (Vaneckova et al., 2008), Russia in 2010

81 (Trenberth and Fasullo, 2012), and China in 2013 (Sun et al., 2014). Socioeconomic  
82 exposure and disaster risks will be magnified in a warmer future (Jones, and O'Neill,  
83 2016; Smirnov et al., 2016), when the more frequent and intense heat extremes of this  
84 century (Fischer and Knutti 2015; Kharin et al., 2013) combine with a greater  
85 population and the accumulation of wealth.

86 In socioeconomic systems, population is most closely related to heat extremes  
87 because of its direct impact on public health (Wang et al., 2019). Various economic  
88 sectors also can be seriously affected by heat extremes, such as agriculture (water  
89 shortages) and industries that rely heavily on hydropower. In addition, tourism,  
90 transportation, construction, and other industries are also affected by heat extremes to  
91 varying degrees (IPCC, 2014). Considering the data on historical damage of heat  
92 extremes (number of people affected, total damage on the economy, etc.) and the  
93 availability of simulated socioeconomic data for the future, we selected population and  
94 economic activity, expressed as GDP, to determine the impact of heat extremes on the  
95 socioeconomic system. Many studies that have quantified future socioeconomic  
96 exposure have not considered changes in populations or GDP but assumed that these  
97 variables remain constant, which is inappropriate for predicting changes in exposure  
98 (Bouwer, 2013; Sun et al., 2017). Most studies have also focused on changes in  
99 exposure based on a specific pathway of emission of a greenhouse gas (GHG) or a  
100 target of global mean temperature (GMT) rise such as 1.5 °C or 2.0 °C (Harrington and  
101 Otto, 2018; Mishra et al., 2017). These analyses of the spatiotemporal variation in  
102 exposure between scenarios and time periods are thus insufficient because the  
103 population and economy (usually calculated by GDP) are both essential elements in  
104 socioeconomic systems and are the factors most severely affected by climatic extremes.  
105 The exposures of populations and GDP are usually predicted separately, and these two  
106 elements are rarely used to assess socioeconomic exposure (Bowles et al., 2014;  
107 Forzieri et al., 2017), although the spatial distributions of populations and economies  
108 are also consistent. Given these factors, we focus in this work on simulating the global  
109 exposure to extreme heat as a function of changes in climate and population or GDP.  
110 The results constitute a first step toward understanding how interactions between  
111 climate change and socioeconomic systems affect exposure patterns.

112 This study systematically quantify the global spatiotemporal distribution of and  
113 changes in exposure of population and GDP to heat extremes under different scenarios  
114 and over different time periods. Bias-corrected projections of five global climate  
115 models (GCMs, Table 1) driven by representative concentration pathways (RCPs) are  
116 used to calculate the frequency of extreme heat events (see Sec. 2.1, Materials).  
117 Combined with population and GDP projections in SSPs (Figs. S1 and S2), which  
118 consider changes in the geographic distribution of population and GDP (see Sec. 2.1,  
119 Materials), the spatiotemporal variation of global exposure to extreme heat of the  
120 population and GDP is quantified in both the base period (1986–2005) and in future  
121 periods (2016–2035 and 2046–2065) under various scenarios (see Sec. 2, Materials and  
122 Methods). We also assess the relative importance of climatic and socioeconomic factors  
123 and their uncertainties to characterize the contribution of climate change and growth in  
124 population and GDP to future changes in extreme-heat exposure. The main target of

125 this study is quantifying the impact of heat extremes on socioeconomic system under  
126 climate change to characterize variation of socioeconomic exposure among scenarios  
127 and periods, distinguish high exposure regions, and identify dominant contributor for  
128 exposure change, so as to support policymakers in the development of climate change  
129 mitigation and adaptation strategies.

## 130 **2 Materials and Methods**

### 131 **2.1 Materials**

132 Daily climatic data were obtained from the Inter-Sectoral Impact Model  
133 Intercomparison Project (ISI-MIP, Warszawski et al., 2014) for the Coupled Model  
134 Intercomparison Project Phase 5 (CMIP5, Taylor et al., 2012) (Table 1), which contains  
135 simulations from five GCMs based on RCPs. The RCP scenarios represent pathways  
136 based on simulated impacts on land use, aerosol emissions, and GHGs (Vuuren et al.,  
137 2011). The four RCPs cover the period up to 2100 and have radiative forcings from the  
138 open literature that vary from 2.6 to 8.5 W/m<sup>2</sup>. The scenarios, RCP2.6, RCP4.5, and  
139 RCP8.5, which represent low, middle, and high GHG emissions, respectively, were  
140 selected for analysis (Vuuren et al., 2011). RCP6.0, which is interpreted as either a  
141 medium baseline or a high-mitigation case between RCP4.5 and RCP8.5, is not used.  
142 The base period was 1986–2005, which is the commonly used reference period in  
143 assessments of projected changes in extreme indices and climate impacts (Schleussner  
144 et al., 2016). Future periods in the 2030s and 2050s were given lengths of 20 years  
145 (2016–2035 and 2045–2065) to be consistent with the base period. The spatial  
146 resolution of the output data was offset-corrected and converted to 0.5° × 0.5° latitude  
147 and longitude by spatial downscaling. Statistical bias-correction methods facilitate the  
148 comparison between observed and simulated data during the historical reference period  
149 and for a continuous transition into the future (Hempel et al., 2013). Preservation of  
150 absolute changes in monthly temperature and relative changes in monthly precipitation  
151 in each grid cell implies that the global warming trend and the climate sensitivities of  
152 the GCMs are preserved, and the trend and the long-term mean are well represented,  
153 which ensures the credibility of the simulated data (Hempel et al., 2013; Warszawski et  
154 al., 2014).

155 The United Nations, the World Bank, and other organizations proposed future  
156 socioeconomic projections for population and GDP. Many previous studies also  
157 combined current socioeconomic data with future climatic data for analysis, although  
158 these studies neglected to consider how changes in socioeconomic factors affect  
159 exposure. We used the predictions of population and GDP from the scenarios of SSPs  
160 based on the selected RCP scenarios. SSPs are reference pathways describing possible  
161 alternative trends in the evolution of societies and ecosystems on a timescale of 100  
162 years without climate change or implementation of climate policies (Riahi et al., 2017).  
163 RCP2.6, 4.5, and 8.5 generally correspond to SSP1, 2, and 3, respectively, based on the  
164 correspondence between the RCPs and SSPs provided by the IPCC (O'Neill et al., 2014,  
165 Table S4). We therefore selected SSP1, 2, and 3 for this study. The RCP2.6-SSP1

166 scenario assumes low carbon emissions, sustainable development proceeding at a  
 167 reasonably high pace, and fewer inequalities. The RCP4.5-SSP2 scenario assumes  
 168 moderate carbon emissions with medium growth in population and GDP. Finally, the  
 169 RCP8.5-SSP3 scenario assumes high carbon emissions with a rapidly growing  
 170 population and a low adaptive capacity. The projections of population and GDP were  
 171 obtained from the National Institute for Environmental Studies, Japan (NIES), which  
 172 were downscaled from the International Institute for Applied Systems Analysis  
 173 (IIASA). The spatial resolution was also  $0.5^\circ \times 0.5^\circ$  latitude and longitude. The  
 174 population and GDP projections were downscaled with explicitly considered spatial  
 175 and socioeconomic interactions between cities, and they used auxiliary variables,  
 176 including road network and land cover. The downscaling results were consistent with  
 177 the scenario assumptions and captured the difference in urban and non-urban areas in a  
 178 more reasonable manner, which ensures the prediction accuracy of the SSPs (Murakami  
 179 and Yamagata, 2016).

180 Table 1. Description of global climate models (GCMs).

Model	Institute	Atmospheric resolution (longitude $\times$ latitude)
GFDL-ESM2M	Geophysical Fluid Dynamics Laboratory	$2.5^\circ \times 2^\circ$
HadGEM2-ES	National Institute of Meteorological Research/Korea Meteorological Administration	$1.875^\circ \times 1.25^\circ$
IPSL-CM5A-LR	Institute Pierre-Simon Laplace	$3.75^\circ \times 1.875^\circ$
MIROC-ESM- CHEM	Japan Agency for Marine-Earth Science and Technology, Atmosphere and Ocean Research Institute (University of Tokyo), and National Institute for Environmental Studies	$2.8^\circ \times 2.8^\circ$
NorESM1-M	Norwegian Climate Centre	$2.5^\circ \times 1.89^\circ$

181

## 182 2.2 Methods

### 183 2.2.1 Hazards of extreme heat

184 Annual days of extreme heat, which is also the frequency of extreme heat, were  
 185 used to quantify the hazard, which is defined as the daily maximum temperature  
 186 exceeding a threshold. The threshold for extreme heat was defined as the 90th percentile  
 187 of daily maximum temperatures for the base period (1986–2005) and was set at  $25^\circ\text{C}$   
 188 when the local 90th percentile was  $<25^\circ\text{C}$  (Garssen et al., 2005). We chose relative  
 189 thresholds rather than a fixed threshold to project global spatiotemporal variation and  
 190 changes in exposure because no single fixed threshold suffices for the substantial  
 191 differences in climatic conditions around the world (Gasparri et al., 2015). Relative  
 192 thresholds were, therefore, the simplest definitions of regionally relevant extreme heat  
 193 around the globe. The frequency of extreme heat was calculated as follows:

$$C = \sum_{i=1}^{365} (TEM_i > THR), \quad (1)$$

$$\bar{C} = \frac{\sum_{j=1}^5 C_j}{5}, \quad (2)$$

194 where  $C$  is the annual number of days of extreme heat (day),  $i$  is the  $i^{\text{th}}$  day of a year,  
 195  $TEM$  is the daily maximum temperature ( $^{\circ}\text{C}$ ),  $THR$  is the local threshold ( $^{\circ}\text{C}$ ),  $\bar{C}$  is the  
 196 multi-model averaged value of  $C$  (day), and  $j$  is the  $j^{\text{th}}$  GCM.

### 197 2.2.2 Exposure to extreme heat

198 We measured population and GDP exposure for each grid cell as the number of  
 199 extreme heat days multiplied by the number of people and GDP, respectively (Jones et  
 200 al., 2015). Therefore, the units of population and GDP exposures are person-days and  
 201 purchasing power parity (PPP) dollar-days, respectively. To calculate exposure in the  
 202 base period and in the future periods (2016–2035 and 2046–2065), we minimized  
 203 interannual variations by using 20-year averages of annual extreme heat days and of the  
 204 projections of population and GDP. The 20-year mean exposure for each projection of  
 205 the five climate models was calculated for the base period and for the future periods.  
 206 Moreover, exposure for the grid cells was also aggregated to global and continental  
 207 scales for further analysis. Explicitly, we have

$$\overline{E_P} = \frac{\sum_{m=1}^{20} C_m \times P}{20}, \quad (3)$$

$$\overline{E_G} = \frac{\sum_{m=1}^{20} C_m \times G}{20}, \quad (4)$$

208 where  $\overline{E_P}$  is the 20-year-averaged population exposure (person-day),  $m$  is the  $m^{\text{th}}$  year  
 209 of the study period,  $C$  is the number of annual days of extreme heat (day),  $P$  is the  
 210 simulated population number (person),  $\overline{E_G}$  is the 20-year-averaged GDP exposure  
 211 (PPP \$-day), and  $G$  is the GDP simulation (PPP \$).

### 212 2.2.3 Analysis of relative importance of change in exposure and cumulative 213 probability

214 Using techniques from a previous study (Jones et al., 2015), we evaluated the relative  
 215 importance of the effects of different factors by categorizing the changes in population  
 216 and GDP exposures in terms of the effects of climate, population, GDP, and interactions.  
 217 The impact of population and GDP was calculated by holding climate constant (i.e., the  
 218 20 year averages of annual days of extreme heat for the base period were multiplied by  
 219 the populations and GDPs in the RCP-SSP scenarios). Population and GDP were  
 220 similarly held constant when calculating the impact of climate (i.e., the population for  
 221 the base period was multiplied by the 20 year averages of annual days of extreme heat  
 222 in the RCP scenarios). The interactive effect was also calculated to determine whether  
 223 the areas with continued population and GDP growth experienced more heat extremes  
 224 under climate change. The changes in population and GDP exposure were categorized



225 as follows:

$$\Delta E_P = C_b \Delta P + P_b \Delta C + \Delta P \Delta C, \quad (5)$$

226

$$\Delta E_G = C_b \Delta G + G_b \Delta C + \Delta G \Delta C, \quad (6)$$

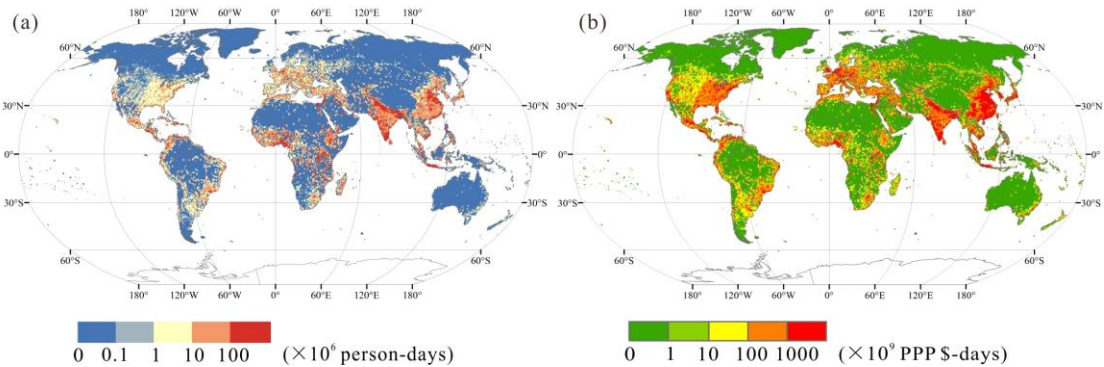
227 where  $\Delta E_P$  is the total change in population exposure,  $\Delta E_G$  is the total change in GDP  
228 exposure,  $C_b$  is the annual days of extreme heat for the base period,  $P_b$  and  $G_b$  are  
229 the population and GDP for the base period, respectively,  $\Delta C$  is the change in annual  
230 days of extreme heat from the base period to future periods, and  $\Delta P$  and  $\Delta G$  are the  
231 changes in population and GDP, respectively, from the base period to future periods.  
232 Therefore,  $C_b \Delta P$  is the population effect,  $C_b \Delta G$  is the GDP effect,  $P_b \Delta C$  and  
233  $G_b \Delta C$  are the climatic effects, and  $\Delta P \Delta C$  and  $\Delta G \Delta C$  are the interactive effects.

234 The uncertainties of changes in population and GDP exposure for future scenarios  
235 were analyzed to evaluate the possible impact of climate change and growth on  
236 population and GDP. The probability analysis of changes in population and GDP were  
237 first separately calculated in each GCM based on the cumulative distribution function  
238 (CDF). Next, the mean value and standard deviation for the five GCMs were computed.  
239 The CDF of a random variable  $X$  represents the probability that  $X \leq x$ .

## 240 3 Results

### 241 3.1 Spatial pattern of population and GDP exposures to extreme heat

242 Figure 1 shows the multi-model average exposures of the population and GDP for  
243 RCP8.5-SSP3 for 2046–2065. Figure S3 shows the frequency of extreme heat, and Figs.  
244 S4 and S5 show the population and GDP exposures, respectively. Tables S1 and S2  
245 present the statistics for population and GDP exposures globally and continentally for  
246 the RCP-SSP scenarios and the different time periods.



247  
248 Fig. 1: Multi-model global projections of average exposures of (a) population and (b)  
249 GDP to extreme heat for the RCP8.5-SSP3 scenario for 2046–2065. PPP is purchasing  
250 power parity in USD.

251 The spatial distribution of the frequency of heat extremes indicates latitudinal  
252 zonation in each time period and for each scenario (Fig. S3). The threshold in the base  
253 period exceeds 25 °C, except at latitudes  $>50^\circ$  and on the Qinghai-Tibet Plateau. Heat  
254 extremes are most frequent near the equator, and their frequency gradually decreased  
255 with increasing latitude in both the base period and future periods. The frequency of

256 extreme heat clearly increases over time. The highest frequency is 36.5 days in the base  
257 period, whereas the frequency is projected to exceed 120 days in the RCP scenarios.  
258 The frequency is significantly higher for 2046–2065 than 2016–2035 under each  
259 scenario. The frequency is highest under the RCP8.5 scenario and lowest under RCP2.6,  
260 but the difference between the scenarios is less than the difference between the time  
261 periods.

262 The regions with high population and GDP exposures to extreme heat are primarily  
263 concentrated in densely populated areas, such as India, China, midwestern Europe, the  
264 eastern USA, and the coastal areas of South America, for both the base period and the  
265 projected scenarios (Fig. 1). Exposure is also high near the equator in Africa because  
266 of the frequent occurrence of extreme heat. Population exposure under the RCP  
267 scenarios is highest for India and the east coast of China ( $>10 \times 10^6$  person-days). GDP  
268 exposure is much higher for eastern China, the Indian subcontinent, western Europe,  
269 and eastern North America than other locations such as northern Asia, northern North  
270 America, and Middle Oceania, with annual GDP exposure  $>100 \times 10^9$  PPP dollar-days.

### 271 **3.2 Global and continental change in exposure to extreme heat**

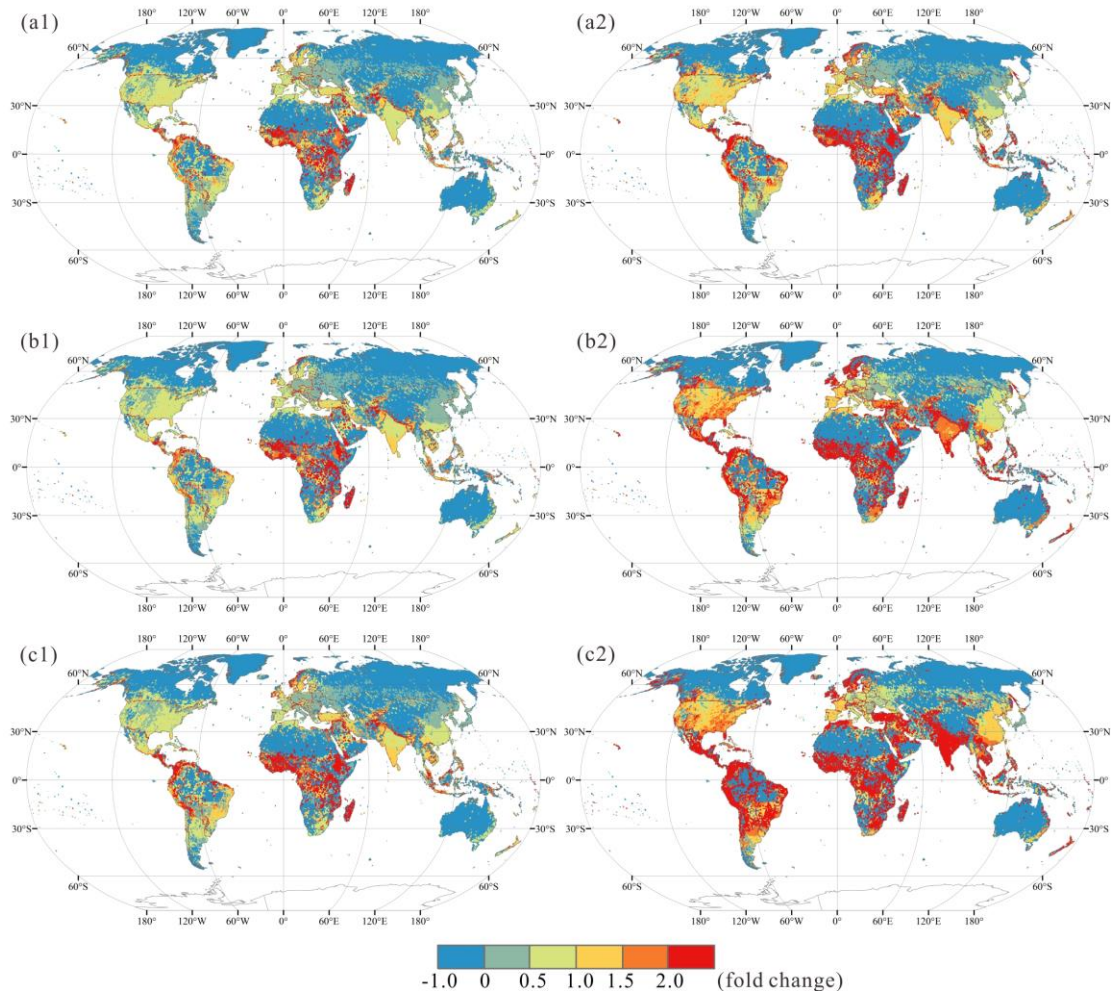
272 Annual exposure of the global population for the base period is  $217.80 \times 10^9$  person-  
273 days, which increases to  $1037.06 \times 10^9$  person-days for 2046–2065 under the RCP8.5-  
274 SSP3 scenario (Table S1). The increase in population exposure is largest for the  
275 RCP8.5-SSP3 scenario and smallest for RCP2.6-SSP1 (Fig. 2). The increase in global  
276 annual GDP exposure is largest for 2046–2065 under the RCP2.6-SSP1 scenario (Fig.  
277 3), with a 10.47-fold increase in exposure relative to the base period (Table S2). In  
278 contrast, the increase is smallest for 2016–2035 under RCP8.5-SSP3, with an increase  
279 of only 3.71-fold relative to the base period. The reason that the highest GDP exposure  
280 appears in the RCP2.6-SSP1 scenario is that SSP1 is a “sustainable” scenario that  
281 assumes economic growth is shared at the global scale, so GDP increases relatively  
282 more in countries that currently have less wealth. Therefore, the exposed GDP at the  
283 global scale is higher in RCP2.6-SSP1, despite the hazard of extreme heat being lower  
284 in RCP2.6.

285 The population exposure is highest for Asia, followed by Africa, and lowest in  
286 Oceania in both the base period and the RCP scenarios. Exposure in Asia and Africa in  
287 the base period is 63% and 14%, respectively (Table S1). The percentage of population  
288 exposure under the three RCP scenarios decreases for Asia and increases for Africa.  
289 The percentage of population exposure for 2046–2065 under the RCP8.5-SSP3  
290 scenario decreases for Asia to 53% and increases for Africa to 29% of global exposure.  
291 Exposure for the continental GDP in the base period ranks as follows: Asia > North  
292 America > Europe > South America > Africa > Oceania (Table S2).

293 The percent of GDP exposure increases for Asia, Africa, and South America and  
294 decreases for North America, Europe, and Oceania. The increase in both continental  
295 population and GDP exposures is largest for Africa, with the annual population  
296 exposure  $>9.20$ -fold higher under the RCP8.5-SSP3 scenario for 2046–2065 than for  
297 the base period, and the change of population exposure is 1.22-fold larger over the same  
298 period and under the same scenarios for Europe than in the base period, which is the

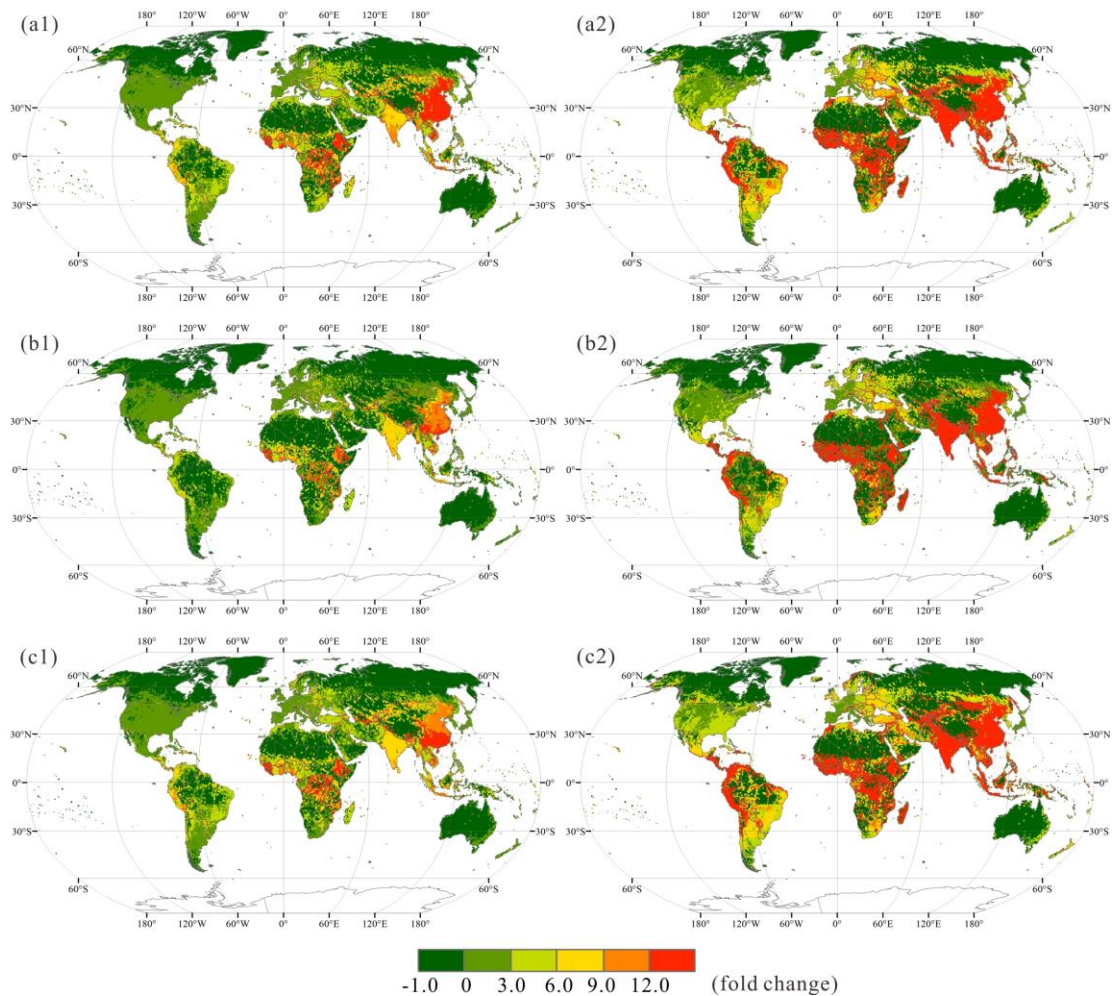
299 smallest change among the continents. GDP exposure increases the most in Africa,  
 300 by >29.34-fold relative to the base period under the RCP2.6-SSP1 scenario for 2046–  
 301 2065, whereas GDP exposure in North America is 3.99-fold higher for 2046–2065 than  
 302 the base period, which is the lowest among continents.

303 Figure 2 presents the relative changes in population exposure for the projected  
 304 scenarios relative to the base period. The rate of change is highest in Africa in regions  
 305 near the equator. Population exposure for 2016–2035 under the RCP2.6-SSP1 scenario  
 306 increases more than 2-fold. The increase in the coastal regions of South America is also  
 307 rapid, by more than 2-fold for 2046–2065 under the RCP4.5-SSP2 scenario. The rate  
 308 of change, however, is <50% in areas where the rate has usually been high, such as  
 309 China, the USA, and Western Europe. Population exposure is much higher for 2046–  
 310 2065 than 2016–2035 under each scenario when the differences are compared between  
 311 different time periods, with time, the population increases gradually, and when that  
 312 increase is crossed with the more frequent heat extremes affected by climate change.  
 313 Population exposure is highest under the RC8.5-SSP3 scenario, where population  
 314 growth is rapid, followed by the RCP4.5-SSP2 and RCP2.6-SSP1 scenarios.



315  
 316 Fig. 2: Multi-model global projections of average relative change in population  
 317 exposure to extreme heat for the three RCP scenarios and two time periods relative to  
 318 the base period: (a) RCP2.6-SSP1, (b) RCP4.5-SSP2, (c) RCP8.5-SSP3, (1) 2016–2035,  
 319 (2) 2046–2065.

320 Figure 3 presents the spatial distributions of the average relative changes in GDP  
 321 exposure for the RCP scenarios projected by multiple models. GDP exposure for 2016–  
 322 2035 increases most rapidly in eastern China, with a more than 9-fold increase relative  
 323 to the base period. GDP exposure also changes for central Africa and the South Asian  
 324 subcontinent, with more than 6-fold increases relative to the base period. GDP exposure  
 325 increases for 2046–2065 relative to the base period and 2016–2035. The increase in  
 326 exposure is largest for Asia and is >12-fold higher than the base period in many  
 327 countries, such as China, India, and Mongolia. GDP exposure also changes for Africa,  
 328 South America, and Eastern Europe. The change in exposure is relatively small for  
 329 North America and Oceania, less than 6-fold relative to the base period. GDP exposure  
 330 is highest under the RC2.6-SSP1 scenario, where GDP growth is fastest, followed by  
 331 the RCP4.5-SSP2 and RCP8.5-SSP3 scenarios.



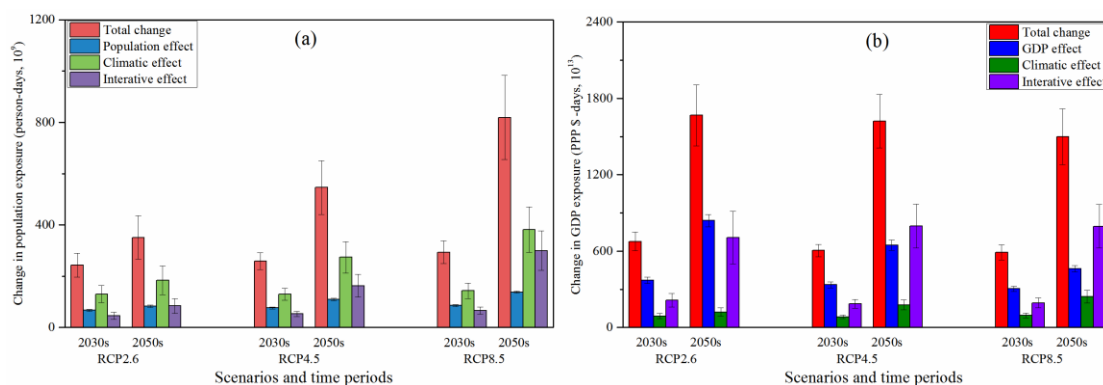
332  
 333 Fig. 3: Multi-model global projections of average relative change in GDP exposure to  
 334 extreme heat for the three RCP scenarios and two time periods relative to the base  
 335 period: (a) RCP2.6-SSP1, (b) RCP4.5-SSP2, (c) RCP8.5-SSP3, (1) 2016–2035, (2)  
 336 2046–2065.

### 337 3.3 Analysis of relative importance of change in exposure

338 To determine the relative importance of various factors, we categorize the changes  
 339 in population and GDP exposures in terms of the effects of population, GDP, climate,

340 and their interactions. Figures 4–6 show the changes in exposure and its components  
 341 for the globe and for the continents under the three RCP scenarios. The change in global  
 342 exposure of the population is primarily affected by the climate, whereas the change in  
 343 global exposure of GDP is mainly attributed to the GDP effect (Fig. 4).

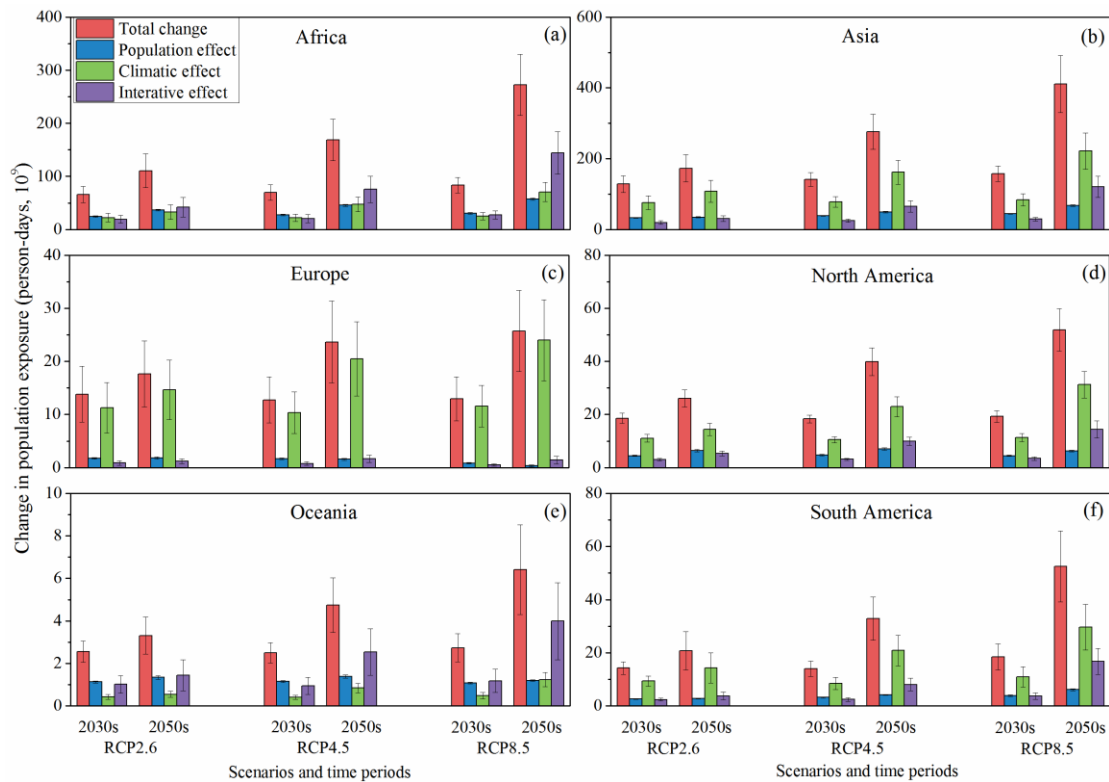
344 The climate effect accounts for nearly half of the total change in population exposure  
 345 (47%–53%) in each scenario and for each period. The effect of population change for  
 346 2016–2035 is larger than the interactive effect, which reverses for 2046–2065. The GDP  
 347 effect is responsible for nearly 50% of the total change in GDP exposure for 2016–2035,  
 348 with approximately 30% and 20% attributable to the effects of climate and interactions,  
 349 respectively. The change in GDP exposure for 2046–2065 under the RCP4.5-SSP2 and  
 350 RCP8.5-SSP3 scenarios is dominated by the interactive effect, at 49% and 53%,  
 351 respectively, followed by the effects of GDP and climate. The increase in the influence  
 352 of the interactive effect highlights the importance of the interactions between GDP and  
 353 climate change in increasing GDP exposure under the scenarios of high GHG emissions.



354

355 Fig. 4: Categorization of projected aggregate global changes in (a) population and (b)  
 356 GDP exposure to extreme heat under the RCP2.6-SSP1, RCP4.5-SSP2, and RCP8.5-  
 357 SSP3 scenarios. Error bars are the standard deviations for the results of the five GCMs.  
 358 PPP is purchasing power parity in USD.

359 The relative importance of the factors of change in population exposure at the  
 360 continental level varies between regions (Fig. 5). As noted above, the percent of  
 361 population exposure worldwide is highest for Asia and Africa, but the dominant  
 362 contribution to the change differs between the two continents. The effect of climate is  
 363 the dominant contribution for Asia, Europe, North America, and South America for all  
 364 scenarios and periods. This result indicates that an increased frequency of heat extremes  
 365 amplifies population exposure, even in the absence of population increases on these  
 366 continents. In contrast, the contribution of the three factors (i.e., the effects of  
 367 population, climate, and the interaction) for Africa is nearly identical for 2016–2035  
 368 because of the strong population increase projected for this continent. The interactive  
 369 effect, however, becomes the primary contribution for 2046–2065, particularly under  
 370 the RCP8.5-SSP3 scenario, accounting for 53% of the total change, which is more than  
 371 the sum of the population and interactive effects. The contributions of the GDP and  
 372 interactive effects for Oceania are nearly the same for 2016–2035 under the three  
 373 scenarios. In contrast, the interactive effect makes the primary contribution to the  
 374 change in GDP exposure for 2046–2065 under the RCP4.5-SSP2 and RCP8.5-SSP3

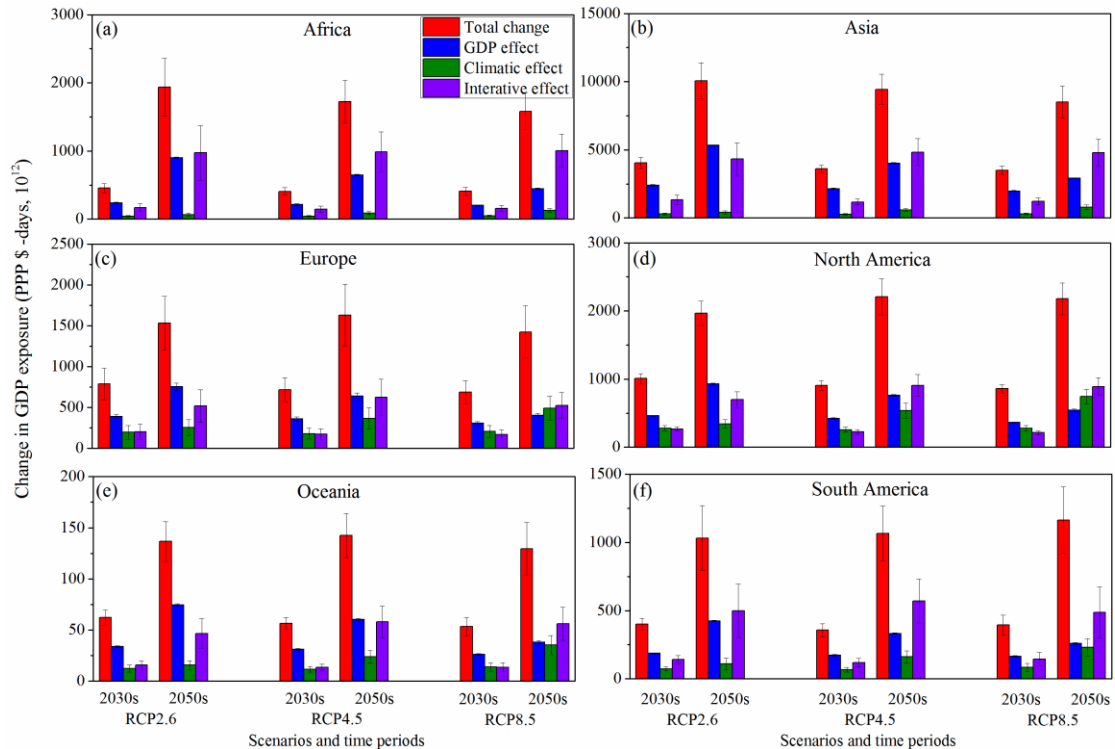


376

377 Fig. 5: Categorization of projected aggregate continental change in population exposure  
 378 to extreme heat under the RCP2.6-SSP1, RCP4.5-SSP2, and RCP8.5-SSP3 scenarios.  
 379 Error bars are the standard deviations for the results of the five GCMs: (a) Africa,  
 380 Asia, (c) Europe, (d) North America, (e) Oceania, (f) South America.

381 Between continents, the differences in relative importance to GDP exposure to the  
 382 effects of GDP, climate, and interactions are clear (Fig. 6), and the contribution of GDP,  
 383 climatic, and interactive effects under the various scenarios and periods also varies  
 384 among continents. The largest contribution for Asia and North America is from GDP  
 385 for 2016–2035 under the three scenarios and for 2046–2065 under the RCP2.6-SSP1  
 386 scenario, whereas the interactive effect is the dominant contribution for 2046–2065  
 387 under the RCP4.5-SSP2 and RCP8.5-SSP3 scenarios. The GDP effect for Africa and  
 388 South America is the primary contributor for 2016–2035, whereas the interactive effect  
 389 is the primary contributor for 2046–2065. The difference between the interactive and  
 390 GDP effects also increases for the pathways involving high GHG emissions in these  
 391 two continents. The interactive effect for the RCP8.5-SSP3 scenario accounts for 64%  
 392 of the total change for Africa, exceeding the contribution of 35% for the GDP effect.  
 393 The interactive effect accounts for 58% of the total change for South America, whereas  
 394 the GDP effect accounts for only 22%. The increase in GHG emissions leading to  
 395 climate change and more frequent heat extremes can account for the increase in the  
 396 difference between the interactive and GDP effects. The interaction between climate  
 397 and change in GDP amplifies the exposure, but the GDP effect decreases, and the  
 398 interactive effect increases as GDP growth slows under the pathways with high GHG  
 399 emissions, which leads to the large difference between the effects under the RCP8.5-  
 400 SSP3 scenario. The GDP effect is the primary contributor for Europe and Oceania for

401 all periods and scenarios, except for 2046–2065 under the RCP8.5-SSP3 scenario,  
 402 which implies that GDP exposure on these two continents would increase quickly  
 403 without the impact of climate change. For almost all continents, GDP exposure is  
 404 dominated by the GDP effect under the RCP2.6-SSP1 scenario because GDP grows  
 405 fastest under this scenario.



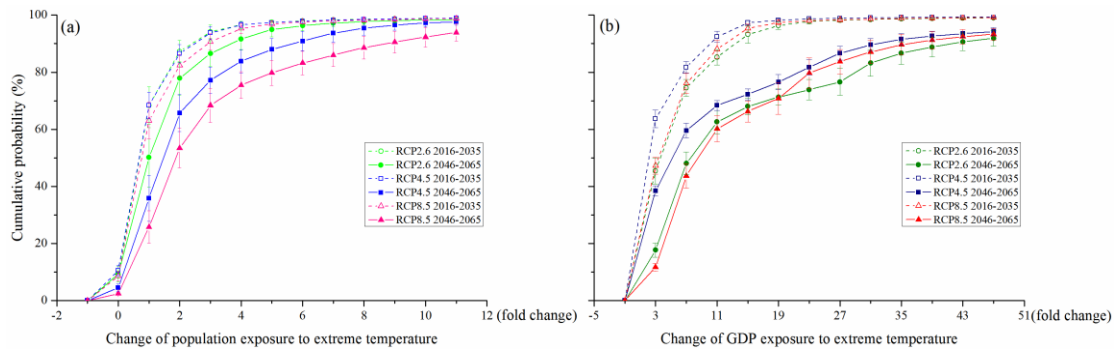
406

407 Fig. 6: Categorization of projected aggregate continental change in GDP exposure to  
 408 extreme heat under the RCP2.6-SSP1, RCP4.5-SSP2, and RCP8.5-SSP3 scenarios.  
 409 Error bars are the standard deviations for the results of the five GCMs. PPP is  
 410 purchasing power parity in USD: (a) Africa, (b) Asia, (c) Europe, (d) North America,  
 411 (e), Oceania, (f) South America.

### 412 3.4 Analysis of cumulative probability of changes in population and GDP 413 exposures

414 Figure 7 shows the cumulative distribution functions for changes in population and  
 415 GDP exposures under the various scenarios and time periods relative to the base period.  
 416 The changes are smaller for 2016–2035 than 2046–2065 for both population and GDP  
 417 exposure, which indicates that population and GDP exposures increase rapidly over  
 418 time, independent of the scenario. Population and GDP exposures, however, differ  
 419 between the three scenarios and the two time periods. The cumulative probability of an  
 420 increase in population exposure is >90% for 2016–2035 and >95% for 2046–2065. The  
 421 change is largest under RCP8.5-SSP3, with 90% probability of a zero- to 10-fold  
 422 increase for both periods, followed by RCP4.5-SSP2 and RCP2.6-SSP1, with a 90%  
 423 probability of a zero- to 7-fold increase relative to the base period. The future increase  
 424 is much faster for GDP exposure than for population exposure because of the faster  
 425 growth in GDP. The change in GDP exposure for 2046–2065 under the RCP2.6-SSP1

426 scenario is the largest among all time periods and scenarios, with 90% probability of a  
 427 difference of -1- to 43-fold, with a 10% probability for an increase >43-fold relative to  
 428 the base period. The increase for 2046–2065 is -1- to 35-fold under RCP8.5-SSP3 and  
 429 -1- to 31-fold under RCP4.5-SSP2 for the same probability. The changes are much  
 430 smaller for 2016–2035 than for 2046–2065, with >70% probability of a zero- to 7-fold  
 431 increase for the three scenarios. The change for 2046–2065 is largest under RCP2.6-  
 432 SSP1, with nearly a 15% probability of a >15-fold increase relative to the base period,  
 433 whereas the increases are 7- and 11-fold under the RCP4.5-SSP2 and RCP8.5-SSP3  
 434 scenarios, respectively, for the same probability.



435

436 Fig. 7: Cumulative probability of projected change in (a) population exposure and (b)  
 437 GDP exposure to extreme heat relative to the base period. Error bars are the standard  
 438 deviations for the results of the five GCMs.

## 439 4 Discussion

### 440 4.1 Impact of a warmer climate on socioeconomic exposure to extreme heat

441 Our study shows spatiotemporal variation and changes in exposure and its  
 442 components at global and continental levels. The results indicate variations among the  
 443 continents (Figs. S4 and S5). For example, population exposure is highest in Asia (Fig.  
 444 S4), accounting for >50% of the global exposure, followed by Africa, North America,  
 445 Europe, South America, and Oceania. The percent of population exposure for Africa  
 446 and South America is projected to increase over time and with an increase in GHG  
 447 emissions, whereas the percentage of population exposure for Asia, Europe, and North  
 448 America is projected to decrease over time. GDP exposure accounted for >50% of the  
 449 total exposure for Asia (Fig. S5), with likely increases under the future scenarios,  
 450 followed by North America, Europe, Africa, South America, and Oceania. The percent  
 451 of exposure for developing countries, such as in Africa and South America, increases  
 452 for the future scenarios. In contrast, decreases would be likely for developed countries,  
 453 such as those in North America, Europe, and Oceania. Extreme heat under climate  
 454 change would thus affect Asia the most, where population and GDP exposures are  
 455 highest. Exposure for Africa is expected to increase rapidly in the future. Therefore,  
 456 more attention should be directed to Asia and Africa for deeper research on extreme  
 457 heat exposure and risk assessment. In addition, the design and implementation of  
 458 effective adaptive measures are urgently needed in regions with high socioeconomic



459 exposure, to lessen populations suffering from heat extremes and reduce the economic  
460 losses under climate change.

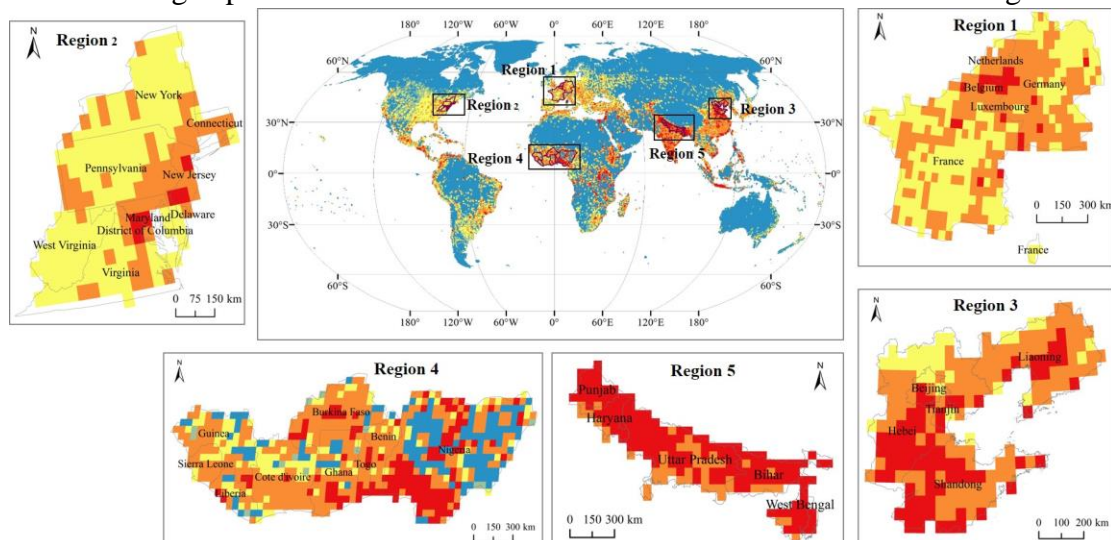
461 We estimate future socioeconomic exposure based on SSP projections with to various  
462 RCP scenarios. Because the current data are well understood and widely accepted,  
463 however, some previous research is based on current spatial distributions and  
464 population and GDP exposures (Hsiang et al., 2017). We also calculate exposure to  
465 future extreme heat regardless of changes in population and GDP (Table S3). The  
466 results indicate that socioeconomic exposure would increase significantly under climate  
467 change, with distinct differences among the RCP scenarios, even if population and GDP  
468 exposures are maintained at current levels. Exposure is lowest under the RCP2.6  
469 scenario and highest under the RCP8.5 scenario. Population and GDP exposures are  
470 1.72- and 1.67-fold higher under RCP8.5 than under RCP2.6, respectively. Both results  
471 for the SSP projections and the current fixed values highlight the importance of  
472 reducing emissions. Overall, it is potential to mitigate the impact of climate change on  
473 both extreme heat hazards and population exposures under the RCP2.6 scenario  
474 compared to RCP4.5 and 8.5 scenarios. And the efficiency of reducing emissions  
475 should be further quantified in future studies under RCP2.6 or other ambitious warming  
476 target, such as 1.5°C and 2°C warming target proposed in Paris Agreement (UNFCCC,  
477 2015), which will be helpful for making climate change mitigation strategies.

#### 478 **4.2 Uncertainty, limitation and further research**

479 Heat extremes could be measured by using different thresholds (e.g., 90, 95, 97.5,  
480 and 99th percentile of daily maximum temperatures over the base period). The spatial  
481 patterns of exposure and change are generally similar, whereas the quantity of exposure  
482 and the relative importance of factors differ greatly (Liu et al., 2017). Assessing  
483 socioeconomic exposure under climate change has many uncertainties, except for the  
484 indices that measure extreme heat. The primary sources of uncertainty include scenarios  
485 of GHG emission (Maurer, 2007), GCMs (Soden et al., 2018), predictions of population  
486 and GDP (Chen et al., 2018) and the calculation method of exposure (Zhang et al.,  
487 2018). The research of Bonan and Doney (2018) on global change in stresses on  
488 terrestrial and marine ecosystems show that the uncertainty on land is mostly from  
489 model uncertainty, which contributes nearly 80% of the total uncertainty in the 21<sup>st</sup>  
490 century. We evaluate population and GDP exposures based on five GCM simulations  
491 after downscaling and assessing the various scenarios and time periods separately.  
492 Figures 4–7 show the differences between the GCMs. In addition to displaying the mean  
493 value of five GCMs, the standard deviation of five GCMs is also displayed as error bars  
494 in the figures. This study generates assessments by considering different sources of  
495 uncertainty, so the results can be considered as reasonable with relatively high accuracy.

496 This study is also subject to some limitations. First, our study quantified  
497 spatiotemporal variation of population and GDP exposures to extreme heat as an  
498 important first step for estimating changes in risk, which made progress compared to  
499 the previous studies ignoring the spatiotemporal variation of the socioeconomic risk  
500 (Barnett et al., 2012; Gasparri and Armstrong, 2011; Voorhees et al., 2011). However,  
501 we do not estimate changes in vulnerability due to the lack of more advanced damage

502 data due to heat extremes. In further studies, we should also concentrate on assessing  
 503 vulnerability when the data are available, which is also essential for assessing risk. In  
 504 addition, adopting measures such as the use of air conditioning and the purchase of  
 505 insurance should be taken into account. These factors would likely improve resilience  
 506 to heat extremes and thus decrease vulnerability and limit the impact of climate change.  
 507 Second, the effect of urban heat islands (UHIs) in addition to global warming is not  
 508 considered explicitly in the climate change simulations in this study. UHIs are  
 509 confirmed to exacerbate the extent and intensity of heat extremes in urban areas and  
 510 increase the risk to urban residents in heat extremes (Dan and Bou-Zeid, 2013; Hajat  
 511 and Kosatky, 2010; Mishra et al., 2015). Recently, as the importance of urbanization in  
 512 climate change has come to be realized, several case studies simulating the impact of  
 513 urbanization on extreme temperature events been done (Chen and Frauenfeld, 2016;  
 514 Grossman-Clarke et al., 2010; Wang et al., 2012). Some research focused on intensely  
 515 urbanized places such as eastern China, the eastern USA, and Western Europe, which  
 516 is consistent with the results of our studies on high-exposure regions. However, some  
 517 other regions such as western Africa and northern India are also expected to suffer high  
 518 exposure to heat extremes in the future. More attention should be focused on these  
 519 regions in future studies (see Fig. 8). However, global studies are rare because of a lack  
 520 of precise land-use and population data. Some other studies assess the future urban  
 521 climate change by using GCM (Fischer et al., 2012; Oleson, 2012). However, given the  
 522 coarse spatial resolution, the influence of GCM on underlying urban surfaces could not  
 523 be fully appreciated, so the impact of future urban development on UHIs was not  
 524 considered in these studies. As a result, the effect of UHIs on extreme temperature  
 525 events may be underestimated. Therefore, in future studies, the design and nesting of  
 526 urban land surface models and the estimation of UHI, especially the heat island  
 527 estimation during heat extremes, should be taken into account, since they are critical  
 528 for estimating exposure and risk to heat extremes in cities due to climate change.



529  
 530 Fig. 8: Regions with high future exposure under climate change. E.g. Western Europe  
 531 (region 1), the eastern USA (region 2), eastern China (region 3), western Africa  
 532 (region 4) and northern India (region 5), may face more risk in heat extremes coupled with the  
 533 effect of urban heat islands in intensely urbanized places.

## 534 **5 Conclusions**

535 This study generated four key findings. First, the regions with the highest population  
536 and GDP exposures to extreme heat are primarily concentrated in densely populated  
537 areas, such as India, China, midwestern Europe, the eastern USA, and the coastal areas  
538 of South America. Second, global population exposure for the years 2046–2065 is  
539 highest under the RCP8.5-SSP3 scenario, with exposure increasing 3.76-fold relative  
540 to the base period 1986–2005. The RCP2.6-SSP1 scenario produces the highest global  
541 GDP exposure, with exposure increasing 10.47-fold for 2046–2065. Third, exposure is  
542 highest for Asia for both population and GDP, which exceeds 50% of the global  
543 exposure. The increase in exposure is largest for Africa, with the annual population and  
544 GDP exposures 9.20- and 29.34-fold higher, respectively, than during the base period.  
545 In contrast, the relative changes in population and GDP exposures are lowest for Europe  
546 and North America, respectively. Fourth, the effect of climate is the dominant  
547 contribution globally to change in population exposure, accounting for nearly half of  
548 the total change (47%–53%). The effect of GDP is responsible for nearly 50% of the  
549 total change in GDP exposure for 2016–2035, whereas the interactive effect makes the  
550 primary contribution for 2046–2065 under the RCP4.5-SSP2 and RCP8.5-SSP3  
551 scenarios, accounting for 49% and 53% of the total change, respectively. In conclusion,  
552 mitigating emissions of greenhouse gases, either at the level of the RCP2.6 scenario or  
553 at a more ambitious target of reduction, is important for reducing socioeconomic  
554 exposure to heat extremes. In addition, designing and implementing effective measures  
555 of adaptation are urgently needed in Asia and Africa to aid socioeconomic systems  
556 suffering from heat extremes due to climate change.

## 557 **Acknowledgments**

558 This study was supported by the National Key Research and Development Program of  
559 China (Grant No. 2016YFA0602402); the Youth Innovation Promotion Association,  
560 CAS (Grant No. 2016049); the Program for “Kezhen” Excellent Talents in Institute of  
561 Geographic Sciences and Natural Resources Research (IGSNRR), CAS, (Grant No.  
562 2017RC101); the Key Research Program of Frontier Sciences, CAS (Grant No.  
563 QYZDB-SSW-DQC005); and the ERC-SyG-2013-610028 IMBALANCE-P. We also  
564 thank ISI-MIP and NIES for data support.

## 565 **References**

- 566 Barnett, A. G., Tong, S. & Clements, A. C. A., 2012. What measure of temperature is  
567 the best predictor of mortality? *Environ. Res.* 118, 149–151.  
568 <https://doi.org/10.1016/j.envres.2010.05.006>
- 569 Bonan, G. B., & Doney, S. C., 2018. Climate, ecosystems, and planetary futures: The  
570 challenge to predict life in Earth system models. *Science*, 359(6375), eaam8328.  
571 doi:10.1126/science.aam8328
- 572 Bouwer, L. M., 2013. Projections of future extreme weather losses under changes in

573 climate and exposure. *Risk Anal.* 33, 915–930. <https://doi.org/10.1111/j.1539->  
574 6924.2012.01880.x

575 Bowles, D. C., Butler, C. D. & Friel, S., 2014. Climate change and health in Earth's  
576 future. *Earths Future* 2, 60–67. <https://doi.org/10.1002/2013EF000177>

577 Burke, M., Hsiang, S. M. & Miguel, E., 2015. Global non-linear effect of temperature  
578 on economic production. *Nature* 527, 235–239.  
579 <https://doi.org/10.1038/nature15725>

580 Carleton, T. A. & Hsiang, S. M., 2016. Social and economic impacts of climate. *Science*  
581 353, aad9837–aad9837. 10.1126/science.aad9837.  
582 <https://doi.org/10.1002/2014GL061859>

583 Ceola, S., Laio, F. & Montanari, A., 2015. Satellite nighttime lights reveal increasing  
584 human exposure to floods worldwide. *Geophys. Res. Lett.* 41, 7184–7190.  
585 <https://doi.org/10.1002/2014GL061859>

586 Chen, J., Liu, Y., Pan, T., Liu, Y., Sun, F., & Ge, Q., 2018. Population exposure to  
587 droughts in China under the 1.5° C global warming target. *Earth Syst Dynam*,  
588 9(3): 1097-1106. <https://doi.org/10.5194/esd-9-1097-2018>.

589 Chen, L. & Frauenfeld, O. W., 2016. Impacts of urbanization on future climate in China.  
590 *Clim dynam* 47, 345–357. <https://doi.org/10.1007/s00382-015-2840-6>

591 Cook, B. I., Smerdon, J. E., Seager, R. & Coats, S., 2014. Global warming and 21st  
592 century drying. *Clim. Dyn.* 43, 2607–2627. <https://doi.org/10.1007/s00382->  
593 014-2075-y

594 Dan, L. & Bou-Zeid, E., 2013. Synergistic Interactions between Urban Heat Islands and  
595 Heat Waves: the Impact in Cities is Larger than the Sum of its Parts. *J Appl*  
596 *Meteorol Clim* 52, 2051–2064. <https://doi.org/10.1175/JAMC-D-13-02.1>

597 Field, C. B., Barros, V. & Stocker, T. F., 2012. Managing the risks of extreme events  
598 and disasters to advance climate change adaptation. Special report of the  
599 Intergovernmental Panel on Climate Change (IPCC). Cambridge University  
600 Press.

601 Fischer, E. M. & Knutti, R., 2015. Anthropogenic contribution to global occurrence of  
602 heavy-precipitation and high-temperature extremes. *Nat. Clim. Change* 5, 560–  
603 564. <https://doi.org/10.1038/nclimate2617>

604 Fischer, E. M., Oleson, K. W. & Lawrence, D. M., 2012. Contrasting urban and rural  
605 heat stress responses to climate change. *Geophys res lett* 39, L03705.  
606 <https://doi.org/10.1029/2011GL050576>

607 Forzieri, G., Cescatti, A., Silva, F. B. E. & Feyen, L., 2017. Increasing risk over time  
608 of weather-related hazards to the European population: a data-driven prognostic  
609 study. *Lancet Planet Health* 1, e200–e208. <https://doi.org/10.1016/S2542->  
610 5196(17)30082-7

611 Garssen, J., Harmsen, C. & De, B. J., 2005. The effect of the summer 2003 heat wave  
612 on mortality in the Netherlands. *Euro. Surveill.* 10, 165–168.  
613 <https://doi.org/10.2807/esm.10.07.00557-en>

614 Gasparrini, A. & Armstrong, B., 2011. The impact of heat waves on mortality.  
615 *Epidemiology* 22, 68–73. <https://doi.org/10.1097/ede.0b013e3181fdcd99>

616 Gasparrini, A. et al., 2015. Mortality risk attributable to high and low ambient

617 temperature: a multicountry observational study. *Lancet* 386, 369–375.  
618 [https://doi.org/10.1016/S0140-6736\(14\)62114-0](https://doi.org/10.1016/S0140-6736(14)62114-0)

619 Grossman-Clarke, S., Zehnder, J. A., Loridan, T. & Grimmond, C. S. B., 2010.  
620 Contribution of land use changes to near-surface air temperatures during recent  
621 summer extreme heat events in the Phoenix metropolitan area. *J Appl Meteorol  
622 Clim* 49, 1649–1664. <https://doi.org/10.1175/2010jamec2362.1>

623 Hajat, S. & Kosatky, T., 2010. Heat-related mortality: a review and exploration of  
624 heterogeneity. *J Epidemiol Commun H* 64, 753–760.  
625 <https://doi.org/10.1136/jech.2009.087999>

626 Harrington, L. J. & Otto, F. E. L., 2018. Changing population dynamics and uneven  
627 temperature emergence combine to exacerbate regional exposure to heat  
628 extremes under 1.5 °C and 2 °C of warming. *Environ. Res. Lett.* 13, 034011.  
629 <https://doi.org/10.1088/1748-9326/aaaa99>

630 Hempel, S., Frieler, K., Warszawski, L., Schewe, J. & Piontek, F., 2013. A trend-  
631 preserving bias correction - the ISI-MIP approach. *Earth Syst Dynam* 4, 219–  
632 236. <https://doi.org/10.5194/esd-4-219-2013>

633 Hirabayashi, Y. et al., 2013. Global flood risk under climate change. *Nat. Clim. Change*  
634 3, 816–821. <https://doi.org/10.1038/nclimate1911>

635 Hsiang, S. et al., 2017. Estimating economic damage from climate change in the United  
636 States. *Science* 356, 1362–1369. <https://doi.org/10.1126/science.aal4369>

637 Huang, J. et al., 2017. Analysis of future drought characteristics in China using the  
638 regional climate model CCLM. *Clim. Dyn.*, 50, 507–525.  
639 <https://doi.org/10.1007/s00382-017-3623-z>

640 IPCC, 2013. *Climate Change 2013: The Physical Science Basis. Contribution of  
641 Working Group I to the Fifth Assessment Report of the Intergovernmental Panel  
642 on Climate Change.* Cambridge, UK, New York, USA: Cambridge University  
643 Press.

644 IPCC, 2014. *Climate Change 2014: Impacts, Adaptation, and Vulnerability. Part A:  
645 Global and 248 Sectoral Aspects. Contribution of Working Group II to the Fifth  
646 Assessment Report of the 249 Intergovernmental Panel on Climate Change.*  
647 Cambridge, UK, New York, USA: Cambridge University Press.

648 Jones, B. & O'Neill, B. C., 2016. Spatially explicit global population scenarios  
649 consistent with the Shared Socioeconomic Pathways. *Environ. Res. Lett.* 11,  
650 084003 (2016). <https://doi.org/10.1088/1748-9326/11/8/084003>

651 Jones, B., O'Neill, B.C., Mcdaniel, L., Mcginnis, S., Mearns, L.O. & Tebaldi, C., 2015.  
652 Future population exposure to US heat extremes. *Nat. Clim. Change* 5, 592–  
653 597. <https://doi.org/10.1038/nclimate2631>

654 Kharin, V. V., Zwiers, F. W., Zhang, X. & Wehner, M., 2013. Changes in temperature  
655 and precipitation extremes in the CMIP5 ensemble. *Clim. Change* 119, 345–  
656 357. <https://doi.org/10.1007/s10584-013-0705-8>

657 King, A. D., Karoly, D. J. & Henley, B. J., 2017. Australian climate extremes at 1.5° C  
658 and 2° C of global warming. *Nat. Clim. Change* 7, 412–416.  
659 <https://doi.org/10.1038/nclimate3296>

660 Liu, Z., Anderson, B., Yan, K., Dong, W., Liao, H. & Shi, P., 2017. Global and regional

661 changes in exposure to extreme heat and the relative contributions of climate  
662 and population change. *Scientific Reports* 7, 43909.  
663 <https://doi.org/10.1038/srep43909>

664 Maurer, E. P., 2007. Uncertainty in hydrologic impacts of climate change in the Sierra  
665 Nevada, California, under two emissions scenarios. *Clim. Change* 82, 309–325.  
666 <https://doi.org/10.1007/s10584-006-9180-9>

667 Mishra, V., Ganguly, A. R., Nijssen, B. & Lettenmaier, D. P., 2015. Changes in observed  
668 climate extremes in global urban areas. *Environ Res Lett* 10, 024005.  
669 <https://doi.org/10.1088/1748-9326/10/2/024005>

670 Mishra, V., Mukherjee, S., Kumar, R. & Stone, D. A., 2017. Heat wave exposure in  
671 India in current, 1.5 °C, and 2.0 °C worlds. *Environ. Res. Lett.* 12, 124012.  
672 <https://doi.org/10.1088/1748-9326/aa9388>

673 Mora, C. et al., 2017. Global risk of deadly heat. *Nat. Clim. Change* 7, 501–506.  
674 <https://doi.org/10.1038/nclimate3322>

675 Murakami, D. & Yamagata, Y., 2016. Estimation of gridded population and GDP  
676 scenarios with spatially explicit statistical downscaling, available at:  
677 <https://arxiv.org/abs/1610.09041>.

678 Nath, R. et al., 2017. CMIP5 multimodel projections of extreme weather events in the  
679 humid subtropical Gangetic Plain region of India. *Earths Future* 5, 224–239.  
680 <https://doi.org/10.1002/2016EF000482>

681 O'Neill, B. C. et al., 2014. A new scenario framework for climate change research: the  
682 concept of shared socioeconomic pathways. *Clim. Change* 122, 401–414.  
683 <https://doi.org/10.1007/s10584-013-0905-2>

684 Oleson, K., 2012. Contrasts between urban and rural climate in CCSM4 CMIP5 climate  
685 change scenarios. *J Clim* 25, 1390–1412. <https://doi.org/10.1175/JCLI-D-11-00098.1>

686

687 Riahi K et al., 2017. The shared socioeconomic pathways and their energy, land use,  
688 and greenhouse gas emissions implications: an overview. *Glob Environ Change*  
689 42:153-168. <https://doi.org/10.1016/j.gloenvcha.2016.05.009>

690 Robine, J. M., Cheung, S. L. K., Roy, S. L., Oyen, H.V., Griffiths, C., Michel, J. P. &  
691 Herrmann, F. R., 2008. Death toll exceeded 70,000 in Europe during the summer  
692 of 2003. *C. R. Biol.* 331, 171–178. <https://doi.org/10.1016/j.crv.2007.12.001>

693 Schlessner, C. F., Lissner, T. K., Fischer, E. M., Wohland, J., Perrette, M., Golly, A.,  
694 Rogelj, J., CHILDERS, K., Schewe, J. & Frieler, K. 2016. Differential climate  
695 impacts for policy-relevant limits to global warming: the case of 1.5 °C and 2 °C.  
696 *Earth Syst Dynam*, 6, 2447–2505. <https://doi.org/10.5194/esd-7-327-2016>

697 Smirnov, O., Zhang, M., Xiao, T., Orbell, J., Lobben, A. & Gordon, J., 2016. The  
698 relative importance of climate change and population growth for exposure to  
699 future extreme droughts. *Clim. Change* 138, 1–13.  
700 <https://doi.org/10.1007/s10584-016-1716-z>

701 Soden, B. J., Collins, W. D. & Feldman, D. R., 2018. Reducing uncertainties in climate  
702 models. *Science* 361, 326–327. <https://doi.org/10.1126/science.aau1864>

703 Sun, H. et al., 2017. Exposure of population to droughts in the Haihe River Basin under  
704 global warming of 1.5 and 2.0°C scenarios. *Quat. Int* 53, 74–84.

705 <https://doi.org/10.1016/j.quaint.2017.05.005>  
706 Sun, Y. et al., 2014. Rapid increase in the risk of extreme summer heat in Eastern China.  
707 Nat. Clim. Change 4, 1082–1085. <https://doi.org/10.1038/nclimate2410>  
708 Taylor, K. E., Stouffer, R. J. & Meehl, G. A., 2012. An overview of CMIP5 and the  
709 experiment design. Bull. Am. Meteorol. Soc. 93, 485–498.  
710 <https://doi.org/10.1175/BAMS-D-11-00094.1>  
711 Trenberth, K. E. & Fasullo, J. T., 2012. Climate extremes and climate change: The  
712 Russian heat wave and other climate extremes of 2010. J. Geophys. Res. Atmos.  
713 117, D17103. <https://doi.org/10.1029/2012JD018020>  
714 UNFCCC Conference of the Parties (COP). 2015. Adoption of the Paris Agreement,  
715 Paris, France.  
716 Vaneckova, P., Beggs, P. J., de Dear, R. J. & Mccracken, K. W., 2008. Effect of  
717 temperature on mortality during the six warmer months in Sydney, Australia,  
718 between 1993 and 2004. Environ. Res. 108, 361–369.  
719 <https://doi.org/10.1016/j.envres.2008.07.015>  
720 Voorhees, A. S., Fann, N., Fulcher, C., Dolwick, P., Hubbell, B., Bierwagen, B. &  
721 Morefield, P., 2011. Climate change-related temperature impacts on warm  
722 season heat mortality: A proof-of-concept methodology using BenMAP.  
723 Environ. Sci. Technol. 45, 1450–1457. <https://doi.org/10.1021/es102820y>  
724 Vuuren, D. P. V. et al., 2011. The representative concentration pathways: an overview.  
725 Clim. Change 109, 5–31. <https://doi.org/10.1007/s10584-011-0148-z>  
726 Wang, J., Feng, J., Yan, Z., Hu, Y. & Jia, G., 2012. Nested high-resolution modeling of  
727 the impact of urbanization on regional climate in three vast urban  
728 agglomerations in China. J Geophys Res: Atmos 117, D21103.  
729 <https://doi.org/10.1029/2012JD018226>  
730 Wang, Y., Wang, A., Zhai, J., Tao, H., Jiang, T., Su, B., ... Fischer, T., 2019. Tens of  
731 thousands additional deaths annually in cities of China between 1.5 °C and  
732 2.0 °C warming. Nature Communications, 10(1), 3376.  
733 <https://doi.org/10.1038/s41467-019-11283-w>  
734 Warszawski, L., Frieler, K., Huber, V., Piontek, F., Serdeczny, O. & Schewe, J., 2014.  
735 The inter-sectoral impact model intercomparison project (ISI-MIP): project  
736 framework. Proc. Natl. Acad. Sci. U.S.A. 111, 3228–3232.  
737 <https://doi.org/10.1073/pnas.1312330110>  
738 Zhang, W., Zhou, T., Zou, L., Zhang, L., & Chen, X., 2018. Reduced exposure to  
739 extreme precipitation from 0.5 °C less warming in global land monsoon regions.  
740 Nature Communications, 9(1), 3153. [https://doi.org/10.1038/s41467-018-](https://doi.org/10.1038/s41467-018-05633-3)  
741 [05633-3](https://doi.org/10.1038/s41467-018-05633-3)  
742 Zhang, Z., Li, N., Xu, H. & Chen, X., 2018. Analysis of the economic ripple effect of  
743 the United States on the world due to future climate change. Earths Future 6,  
744 828–840. <https://doi.org/10.1029/2018EF000839>